Chinese Chemical Letters 35 (2024) 109298

Contents lists available at ScienceDirect

Chinese Chemical Letters

journal homepage: www.elsevier.com/locate/cclet

Size-controlled synthesis and near-infrared photothermal response of Cp* Rh-based metalla[2]catenanes and rectangular metallamacrocycles

Ying Zhao[a,1], Yin-Hang Chai[a,b,1], Tian Chen[a], Jie Zheng[a], Ting-Ting Li[a], Francisco Aznarez[c], Li-Long Dang[a,c,*], Lu-Fang Ma[a,b]

[a] College of Chemistry and Chemical Engineering, Henan Key Laboratory of Function-Oriented Porous Materials, Luoyang Normal University, Luoyang 471934, China
[b] College of Chemistry, Zhengzhou University, Zhengzhou 450001, China
[c] Shanghai Key Laboratory of Molecular Catalysis and Innovative Materials, State Key Laboratory of Molecular Engineering of Polymers, Department of Chemistry, Fudan University, Shanghai 200438, China

ARTICLE INFO

Article history:
Received 20 September 2023
Revised 30 October 2023
Accepted 9 November 2023
Available online 13 November 2023

Keywords:
[2]Catenanes
Photothermal materials
Supramolecular topologies
Half-sandwich fragment
3,3′-N-donor analogues

ABSTRACT

A variety of research reports on novel supramolecular topologies have been published over the last years. However, it is still a great challenge to tap into the inner functional properties of these complexes. Herein, two tetranuclear metallamacrocycles **1** and **2** and four octonuclear [2]catenanes **3**–**6** were constructed successfully *via* a coordination-driven self-assembly strategy, by conscious design and use of the tetramethyl bidentate pyridine ligand **L1**, and the appropriate selection of six binuclear half-sandwich rhodium building units with different longitudinal dimensions. The complexes have been fully characterized by single crystal X-ray diffraction analysis and NMR spectroscopy. Furthermore, near-infrared photothermal studies of the obtained [2]catenanes reveal different photothermal response in solid and solution states, which may be attributed to a strong fluorescence quenching effect of the half-sandwich organometallic fragment and different conjugated effect of Cp*Rh based building blocks in the interlocking structures. The photothermal conversion efficiencies of [2]catenanes **4**–**6** fall in the range 30.5%–16.5% respectively. This contribution aims to play a key role in the experimental development of Cp*-based photothermal materials.

Supramolecular compounds including organometallic fragments have attracted increasing attention during recent years, not only due to their unique topological structures, but also owing to their possible application in the fields of molecular machinery, photoelectric materials or biological simulation [1–10]. Supramolecular complexes such as organometallic macrocycles [11,12], metallacages [13–20], [1–5]catenanes [21], Borromean rings [22], Solomon links [23], and knots and ravels [24] can be mainly constructed by following two synthetic strategies. (a) Metal-cation template method: it is one of the earliest synthetic methods and allowed the successful synthesis of a remarkable number of organometallic compounds with complicated topologies [25–27]. (b) Coordination-driven self-assembly method: it has proven to be a powerful the coordination-driven self-assembly strategy. They contributed significantly to the isolation and characterization of unprecedented knots, rings, chains and other supramolecular compounds [28]. In addition, Stang [29], Fujita [30], and Raymond [31] have independently developed new methods leading to the self-assembly of discrete metallacycles and metallacages with well-defined shapes and dimensions. Recently, the coordination-driven self-assembly of half-sandwich based organometallic fragments (Rh or Ir) with designed functionalized ligands has shown a straightforward way for the rational design of supramolecular complexes [32–36]. Thus, Jin obtained a Borromean ring based on three metallarectangles through a template-free, all-in-one self-assembly [37].

A variety of highly complex structures, including metalla[2–4]catenanes, Borromean rings, Solomon links or various knots, have been obtained by using half-sandwich rhodium or iridium fragments. These studies mainly use 4,4′-N donor dipyridine-based ligands due to their uniform charge distribution and symmetrical coordination ability [38–40]. In comparison, the 3,3′-N- or 2,2′-N-donor analogues, endowed with asymmetric charge distribution, cannot easily form stable π-π stacking interactions with charge-rich conjugate planes. Therefore, research on their application in

* Corresponding author.
E-mail address: danglilong8@163.com (L.-L. Dang).
[1] These authors contributed equally to this work.

https://doi.org/10.1016/j.cclet.2023.109298
1001-8417/

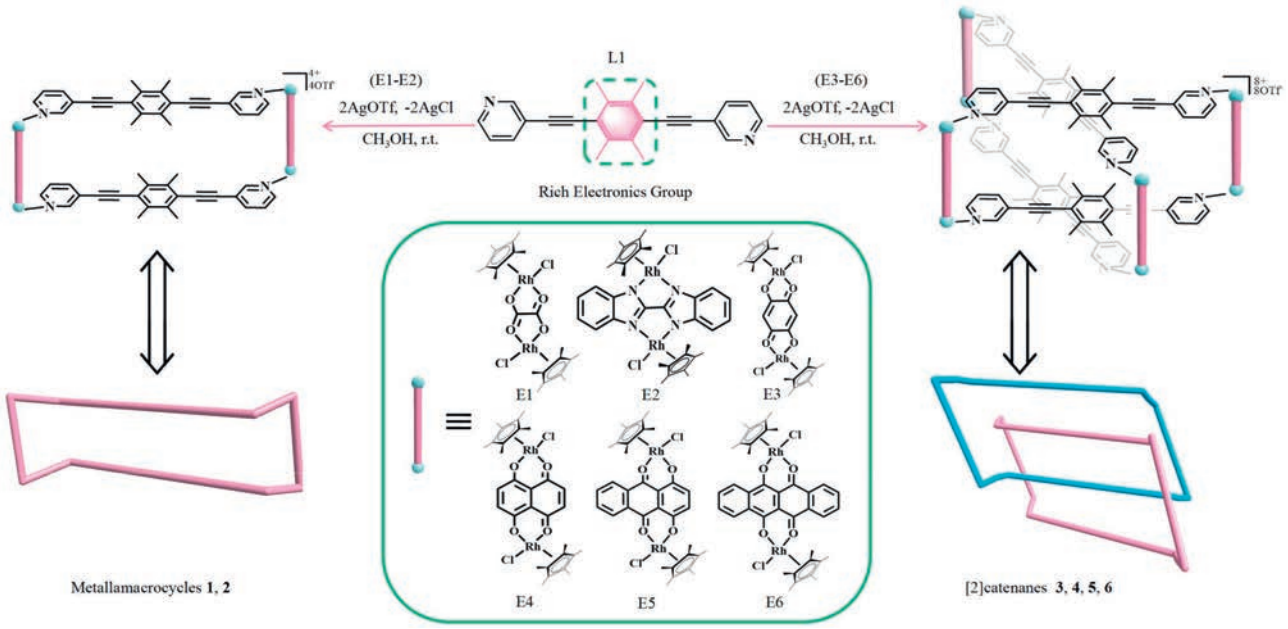

Scheme 1. The synthesis process of organometallic supramolecular compounds and dinuclear building blocks **E1**-**E6** used in this work for coordination-driven self-assembly studies.

the synthesis of supramolecular organometallic compounds is still a major scientific problem.

While the synthesis of unprecedented organometallic supramolecular compounds is a field in continuous development, almost no investigation of potential applications involving these structures has been carried out [41–45]. Organometallic compounds have been of interest to researchers for their applications in photothermal therapy and photothermal/photoacoustic imaging [46–48]. In order to obtain materials with higher photothermal conversion, it is important to consider two aspects: (a) to enhance the infrared absorption by increasing the conjugated plane length or π-π packing double number, (b) to inhibit the radiation transition process by enhancing the quenching effect [49]. We decided to explore the photothermal conversion ability of organometallic supramolecular compounds with different π-π stackings.

A series of compounds based on Cp*Rh fragments with different π-π stacking interactions have been constructed using the size effect. Therefore, a 3,3′-((2,3,5,6-tetramethyl-1,4-phenyl)-di(acetylene 2,1-diyl))dipyridine ligand (**L1**, strong electron-rich center) has been synthesized. Six Cp*Rh building blocks with different longitudinal sizes (**E1**-**E6**) (Scheme 1) were selected to construct two types of supramolecular topologies: metallamacrocycles and metalla[2]catenanes. First, the self-assembly of ligand **L1** and building units **E1**, **E2** (Rh-Rh non-bonding distances: 5.53 and 5.58 Å) has been investigated. Two metallamacrocycles were obtained, thereby supporting our assumption that the short length hampers stacking interactions. As expected, the combination of **L1** with **E3**, **E4**, **E5** or **E6** formed four stable metalla[2]catenanes, most likely due to the suitable Rh-Rh non-bonding distance in these complexes (7.96–8.30 Å). Remarkably, the strong electron-rich unit in the central part of **L1** is prone to form self-stacking interactions, promoting non-radiative transition, and thereby leading to good photothermal conversion performance in both solution and solid state. Studies have shown that, in addition to the stacking interactions promoted by the central unit of **L1**, the conjugated effect of the building units also plays an important role in the process of photothermal conversion. Recorded data indicate that the compounds **3**, **4**, **5** and **6** displayed different photothermal conversion ability based on **E3**-**E6**. The [2]catenane **4** displayed the best photothermal conversion efficiency possibly due to suitable building block size and strong conjugated effect (30.5%). Thus, the photothermal conversion efficiency of metalla[2]catenanes **5** and **6** falls in the value 17.1%−16.5%. In summary, this contribution shows that the change of the longitudinal dimensions and different conjugated characteristic of Cp*Rh building blocks lead to formation of interlocked organometallic supramolecular compounds and special photothermal conversion efficiency.

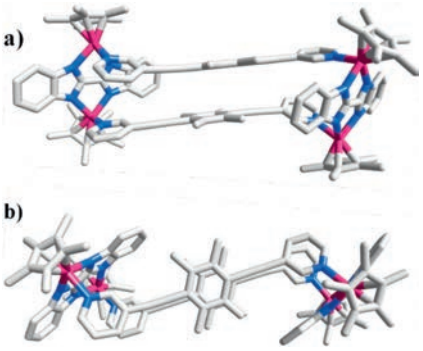

Fig. 1. (a) Side view and (b) top view of the molecular structure of **2**.

Firstly, self-assembly of tetranuclear metallamacrocycles **1** and **2**, based on **E1** and **E2**. Building blocks **E1** ($Cp^*_2Rh_2(\mu$-η^4-$C_2O_4)]Cl_2$) and **E2** ($[Cp^*_2Rh_2(BiBzlm)]Cl_2$) were selected to react with ligand **L1**. As expected, two tetranuclear metallamacrocycles were obtained in high yields (87.4% and 86.5%).

The structure of the complexes was determined by single crystal X-ray diffraction analysis, NMR spectroscopy and ESI-TOF-MS.

Single-crystal X-ray diffraction analysis of complex **2** revealed the structure of the complex in the solid state. Two binuclear $[Cp^*_2Rh_2(BiBzlm)]^{2+}$ cations are connected by two ligands **L1**, thus forming a tetranuclear metallamacrocycle (Fig. 1). A detailed analysis of the molecular structure of complex **2** revealed that the central distance between the two ligands **L1** is 3.79 Å. Interestingly, the short distance clearly hampers the formation of interlocking

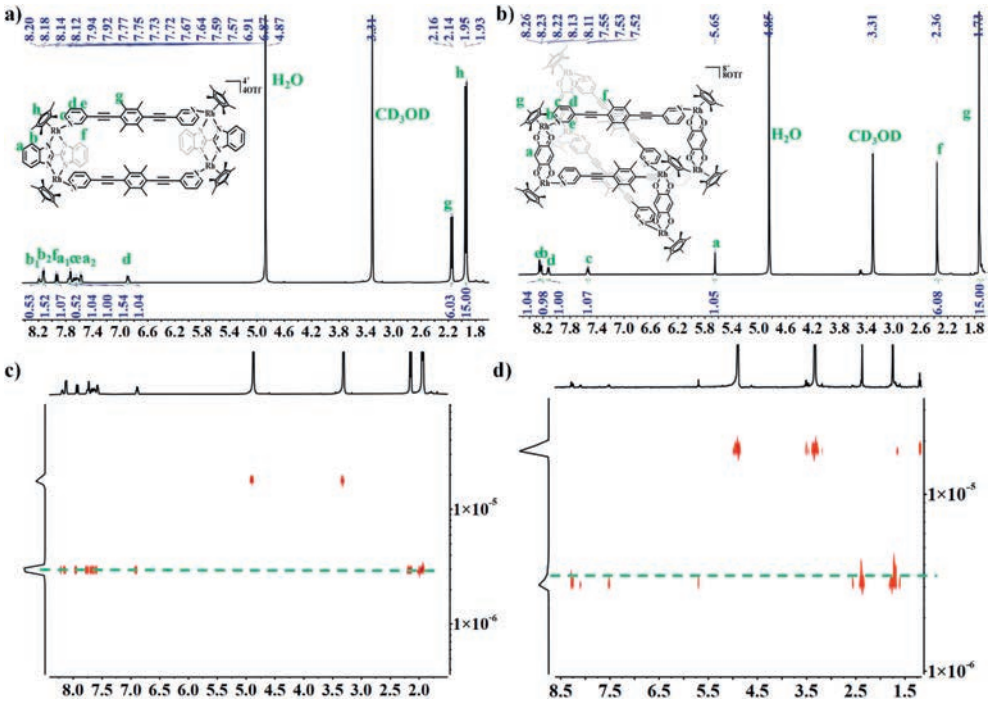

Fig. 2. ^{1}H NMR (500 MHz, CD_3OD) spectra of (a) tetranuclear metallamacrocycle **2** and (b) [2]catenane **3** (CD_3OD, $\delta = 3.31$ ppm). ^{1}H–^{1}H DOSY NMR (500 MHz, CD_3OD) spectra of (c) tetranuclear metallamacrocycle **2** (2.88×10^{-6} cm^2/s) (12.5 mmol/L, with respect to Cp*Rh) and (d) [2]catenane **3** (3.18×10^{-6} cm^2/s) (18.4 mmol/L, with respect to Cp*Rh).

complexes. In addition, the molecular structure of **2** exhibits a Z-shape. In an effort to study the behavior of complex **2** in solution, NMR spectra of **2** in CD_3OD were recorded and analyzed. The ^{1}H NMR spectrum of complex **2** showed a singlet at δ 1.95, which has been attributed to the resonance of the protons belonging to the Cp* group. Furthermore, the doublet at δ 2.16 belongs to the -CH_3 protons of ligand **L1**. While the aromatic protons of **L1** appeared at δ 6.90, 7.68, 7.75 and 7.95 ppm, the resonances of the protons of **E2** appeared as two sets of multiplets at δ 8.23–8.12. ^{1}H–^{1}H COSY NMR spectroscopy confirmed the proton-assigned resonances (Fig. 2a and Fig. S5 in Supporting information). Finally, the ^{1}H–^{1}H DOSY NMR spectrum of **2** revealed a single diffusion coefficient according with the formation of a tetranuclear metallamacrocycle in solution ($D = 2.88 \times 10^{-6}$ cm^2/s) (Fig. 2c).

Moreover, the recorded NMR spectra of complex **1** are very similar to those of complex **2** (Figs. S2-S4 in Supporting information). Complex **1** is also a simple metallamacrocycle. The structure of complexes **1** and **2** was also confirmed by ESI-TOF-MS, which revealed specific valence states at *m/z* 650.11 and 746.17, corresponding to $[\mathbf{1}-3OTf]^{3+}$ and $[\mathbf{2}-3OTf]^{3+}$, respectively (Figs. 3a and d), in good agreement with the calculated theoretical distributions.

Secondly, self-assembly of metalla[2]catenane complexes **3**, **4**, **5** and **6**, based on **E3-E6**. Owing to our desire to obtain and study interlocking structures, a series of experiments were conducted by using the longer building blocks **E3**, **E4**, **E5** and **E6**, and ligand **L1**. Thus, four metalla[2]catenane complexes **3**, **4**, **5** and **6** were obtained, and their structure was confirmed by NMR spectroscopy and single crystal X-ray diffraction analysis.

The NMR spectra of complexes **3**, **4**, **5** and **6** in CD_3OD were firstly studied. The ^{1}H NMR spectrum of **3** in CD_3OD showed two singlets at δ 8.26 and 2.36 ppm, corresponding to the pyridinyl and -CH_3 group protons of ligand **L1**. Furthermore, the doublets at δ 8.22 and δ 8.13, and the multiplet at δ 7.52–7.55 were assigned to the protons of the pyridinyl ligand **L1**. The resonances from the protons of 2,5-dihydroxy-1,4-benzoquinon appeared as a singlet at δ 5.65 (Fig. 2b). The ^{1}H–^{1}H COSY NMR spectra of **3** supports the resonances assignment (Fig. S6 in Supporting information), while the ^{1}H–^{1}H DOSY NMR spectra of **3** revealed a single diffusion coefficient ($D = 3.18 \times 10^{-6}$ cm^2/s), indicating that only one assembled stoichiometry appears in solution (Fig. 2d). Similar spectra were obtained and studied for complexes **4**, **5**, **6**, typical of metalla[2]catenanes. The NMR spectra of complex **4** are very similar to those of complex **3**. However, note that a resonance belonging to an **E4** proton appeared at δ 7.19. In addition, ^{1}H–^{1}H DOSY NMR spectra ($D = 3.11 \times 10^{-6}$ cm^2/s) were used to determine the single diffusion coefficient of **4** (Figs. S8-S10 in Supporting information).

Subsequently, ^{1}H–^{1}H COSY and ^{1}H–^{1}H DOSY NMR spectra were used to assign proton signals in the ^{1}H NMR spectra of **5** and **6** (Figs. S14, S15, S20 and S21 in Supporting information). The position of the proton signals of **L1** in complexes **5** and **6** is similar to that of the protons in **3** and **4**. Interestingly, the signals belonging to the protons in the Rh^{III} building block **E5** appeared at δ 7.98, 8.62–8.64 and 7.24 ppm.

Similarly, the signals corresponding to the protons of the Rh^{III} block **E6** appeared at δ 7.98–8.00 and 8.68–8.69 ppm. Furthermore, the ^{1}H–^{1}H DOSY NMR spectra of complexes **5** and **6** showed diffusion coefficients of 3.13×10^{-6} cm^2/s and 3.01×10^{-6} cm^2/s, respectively, indicating that there is only one complex in solution (Figs. S16 and S22 in Supporting information). Slow diffusion of isopropyl ether into methanolic solutions of compounds **3**, **4**, **5** or **6** led to the isolation of single crystals of **3**, **4** and **5** Subsequently, single crystal X-ray diffraction analysis confirmed their precise structures in the solid state.

Complexes **3**, **4** and **5** are discrete interlocking metalla[2]catenanes in the solid state (Figs. 4 and 5, Fig. S1 in Supporting information). The molecular structure of complex **3** was refined in the *P*-1 space group, and subsequent close contact analysis showed that **3** is stabilized by interactions between the tetramethyl phenyl group of **L1** in the two metallamacrocycles and the pyridyl group in **L1** (Figs. 4a, c and d). In contrast with the molecular structure of **3**, complex **4** is stabilized by strong sandwich-type π-π stacking interactions between the four phenyl

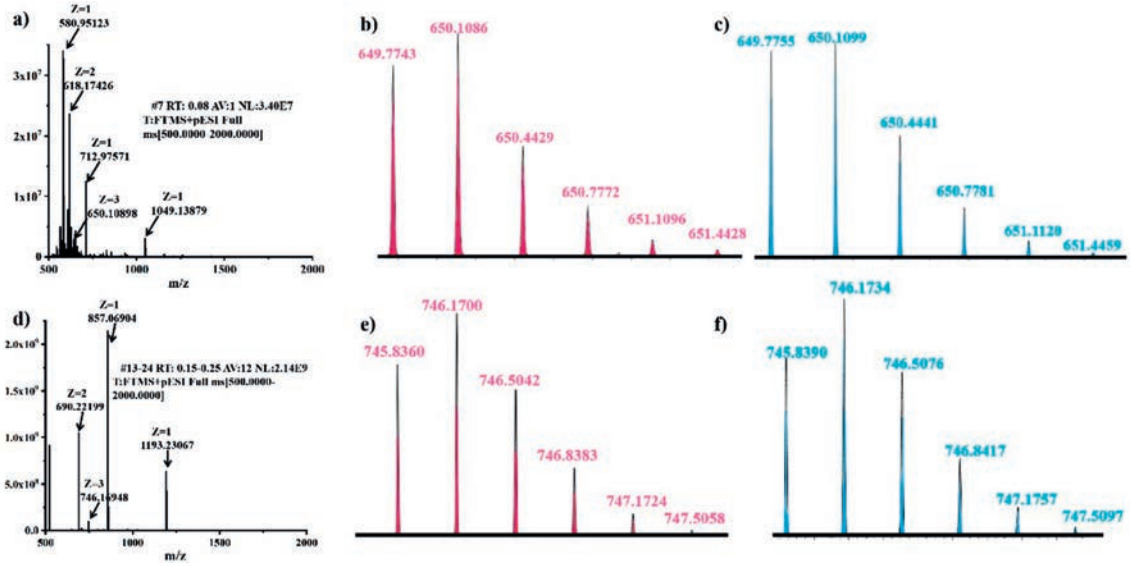

Fig. 3. (a, d) ESI TOF-MS spectra of tetranuclear metallarectangles **1** and **2**. (b, e) Experimental (top) and calculated (below) (3^+ mass peak of **1**) and (c, f) experimental (top) and calculated (below) (3^+ mass peak of **2**).

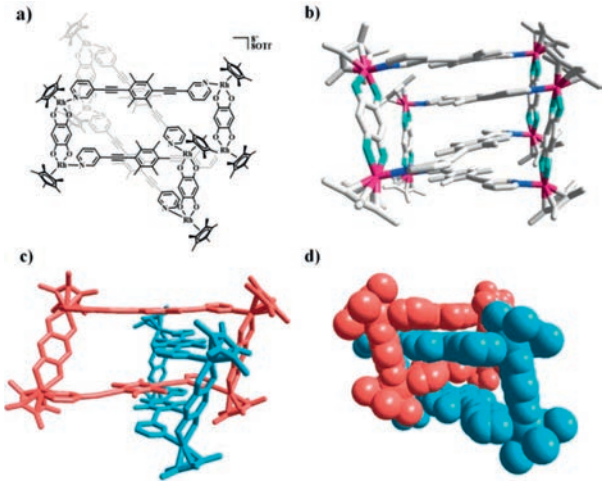

Fig. 4. (a) Chemical structure of [2]catenane **3**. (b) Solid-state structure of **3**, showing the $\pi-\pi$ stacking interactions. (c, d) Two-colors solid-state structure of metalla[2]catenane **3**.

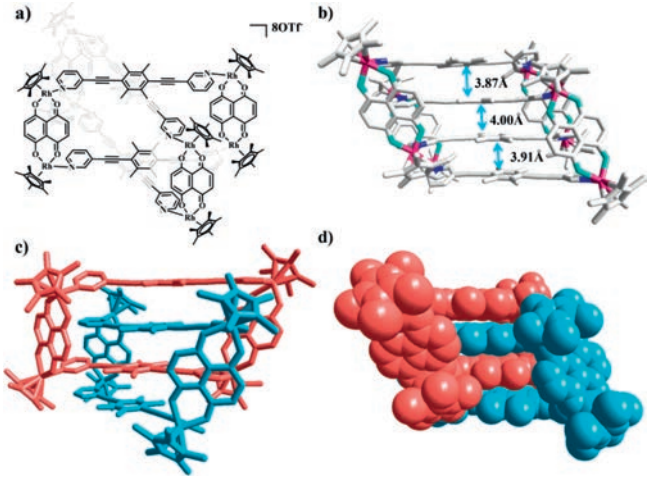

Fig. 5. (a) Chemical structure of [2]catenane **4**. (b) Solid-state structure of **4**, showing the $\pi-\pi$ stacking interactions. (c, d) Two-colors solid-state structure of metalla[2]catenane **4**.

groups of **L1** in the two metallamacrocycles with distances between the benzene ring planes of 3.87, 4.00, and 3.91 Å (Figs. 5b-d). In addition, metalla[2]catenanes **5** is very similar in structure to metalla[2]catenanes **4**, except that the different conjugated units are replaced in the same place (Fig. S1).

In order to perform further experiments, the stability of [2]alkane **3–6** was studied. Previous research contributions in the field have shown that addition of polar solvents, concentration reduction, or addition of suitable guest molecules can result in efficient structural conversion of complicated interlocking structures into simple metalla-macrocycles [50–53]. In an effort to study the use of induced effects to cause the conversion of the obtained [2]catenanes into hard-to-obtain metalla-macrocycles, different experiments were performed. Interestingly, no interconversion was observed by means of these methodologies. Remarkably, the addition of pyrene to methanolic solutions of complex **3** or **4** had no effect on the structure of the [2]catenanes.

The observed outstanding structural stability of [2]catenanes **3** and **4** is very rare for interlocked compounds (Fig. 6, Figs. S7, S11-S13 in Supporting information). Similar research with complexes **5** and **6** (addition of pyrene molecules, addition of DMF or solvent concentration changes) led to the same observation, thereby highlighting the astonishing solvent-, concentration- and guest-stability of the [2]catenane compounds **5** and **6** (Figs. S17-S19, S23 and S24 in Supporting information). The rare structural stability of metalla[2]catenanes **3**, **4**, **5** and **6** encourages us to further study their properties in future research Furthermore, we decided to investigate their photothermal conversion properties.

Recently, near-infrared photothermal conversion (NIR) has been widely used in these fields of photodynamic therapy, photothermal sensing and photocatalysis, *etc.* [46,54–60]. The common law of synthesizing efficient near-infrared photothermal materials is to increase near-infrared absorption and reduce the radiation transition process.

In this study, the metallamacrocycles **1–2** and metalla[2]catenanes **3–6** are discrete structures with sequentially varying near-infrared absorption based on Rh-based modules of different conjugate planes. The NIR absorption intensity and differ-

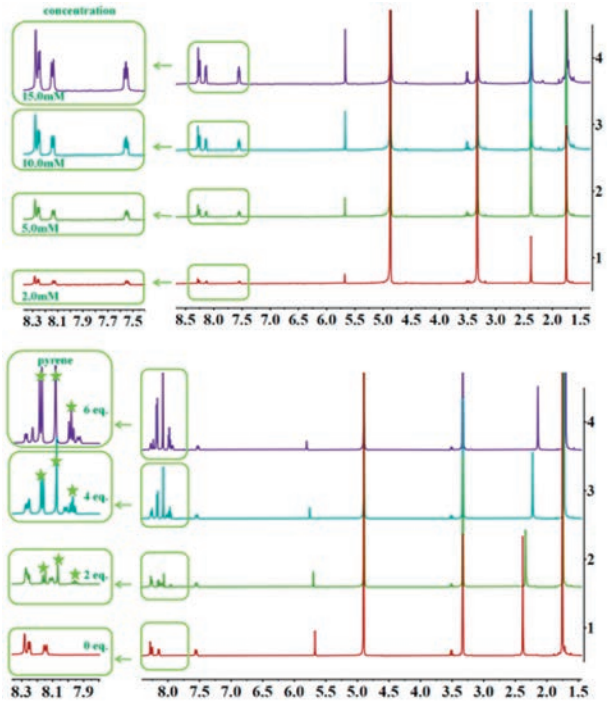

Fig. 6. ^{1}H NMR (500 MHz, CD_3OD, ppm) spectra of **3**. (a) Spectral changes under concentration effects (15.0–2.0 mmol/L). (b) Changes of nuclear magnetic hydrogen spectrum induced by pyrene molecular content.

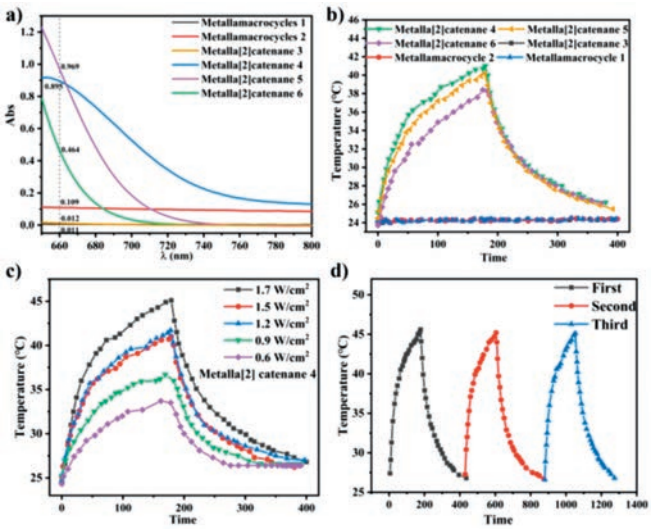

Fig. 7. (a) Absorption of discrete structures **1**–**6** in the near infrared region (700~650 nm). (b) Photothermal conversion curves of supramolecular structures **1**–**6** under laser irradiation of 0.6 W/cm^2. (c) Near-infrared photothermal conversion curves of metalla[2]catene **4** at 660 nm by 0.3, 0.6, 0.9 W/cm^2 [2]catene **4** under 0.9 W/cm^2 laser irradiation. (d) Cyclic photothermal conversion curves.

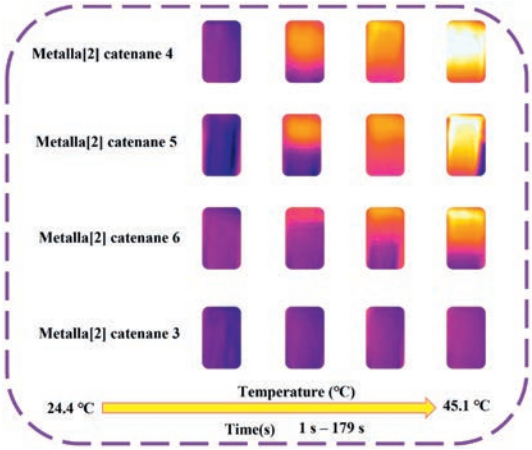

Fig. 8. (a) Near infrared thermal imaging of [2]catenanes **3**–**6** performed in a specific container under 660 nm laser irradiation.

ent π-π stacking interactions in the structure play an important role in the photothermal conversion process. We used [2]catenanes **3–6**, endowed with similar π-π packing interaction in solid state (Figs. 4 and 5), and two metallamacrocycles **1–2**, with a single π-π packing interaction in solid state (Fig. 1). The same number of conjugated planes is guaranteed by controlling the molar ratio of the metallamacrocycles **1** and **2** to metalla[2]catenane **3–6** to 2:2:1:1:1:1. Subsequently, corresponding amounts of discrete structures **1–6** were dissolved in 3 mL of methanol for UV–vis absorption experiments. The results showed that compounds **1–6** had absorbance values at 660 nm (**1**: $A = 0.011$; **2**: $A = 0.109$; **3**: $A = 0.012$, **4**: $A = 0.895$, **5**: $A = 0.969$, **6**: $A = 0.464$) (Fig. 7a).

In addition, according to the absorption range of the solution ultraviolet, a laser lamp with a wavelength of 660 nm was chosen to irradiate samples, and these corresponding solutions of 1 mL were taken into a specific container for work, respectively. The near-infrared photothermal conversion curves of the two metallarectangles **1** and **2** showing the specific heating process were obtained. However, metallarectangles **1** and **2** showed little change in temperature, suggesting that the single π-π packing interaction found in solids may not exist in solution possibly due to dynamic twisting caused by the uncontrollability of the ligand. Metalla[2]catenanes **3–6** showed a different and obvious warming process (Figs. 7b and 8). While the [2]catenane **3** showed small warming trend, [2]catenane **4** (from 25.1 °C to 41 °C), **5** (from 25.5 °C to 40.2 °C) and **6** (from 24.4 °C to 38.4 °C) exhibited remarkable temperature changes (1.5 W/cm^2), enabling the calculation of a photothermal conversion efficiency (details are shown in Supporting information) of 18.8% (**4**), 17.1% (**5**), 16.5% (**6**) (Figs. S31, S33 and S34 in Supporting information). Note that these values are higher than those of reported organic D–A cocrystal materials [43]. This enhanced photothermal temperature and outstanding photothermal conversion of metalla[2]catenanes **4**, **5** can be attributed to the synergistic effect of π-π stacking, conjugated effect of building blocks and the fluorescence quenching effect from Cp*Rh fragments. The weak conjugation effect of building unit **E3** triggers extremely poor photothermal conversion of [2]catenane **3**. The proper conjugation effect and size of building block **E4** result in the best photothermal conversion effect.

The remarkable photothermal conversion performance of [2]catenane **4** prompted us to study the conversion efficiency at different powers. Recorded data shows that a power increase from 0.6 W/cm^2 to 1.7 W/cm^2 results in an increase of the temperature (Fig. 7c). The [2]catenane **4** exhibits the largest temperature change under a power of 1.7 W/cm^2 (temperature rise from 24.5 °C to 45.1 °C). Remarkably, the efficiency of the photothermal conversion decreases with the increase of power from 30.5% to 16.1% (Figs. S28-S32 in Supporting information). Considering that cyclic stability is a major indicator to determine the quality of materials, we selected the metalla[2]catenane **4** to carry out three cycles at a power of 1.5 W/cm^2. Obtained results show that similar temperature change can be achieved with small error. Furthermore, the near-infrared photo-thermal conversion of the [2]catenane **4–6** series in solid state has also been studied. Solid UV–vis spectrum studies (Fig. 9a) showed that compounds **4–6** have absorbance values at 730 nm of 0.868 (**4**), 0.481 (**5**) and 0.392 (6). The pho-

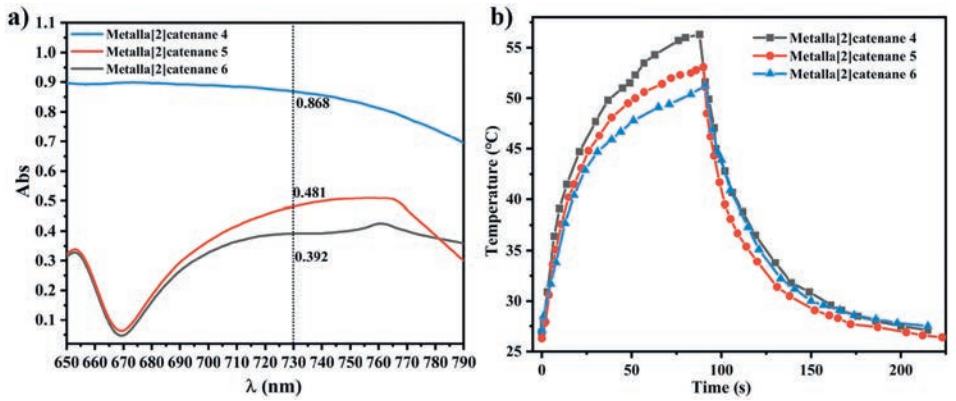

Fig. 9. (a) Absorption in the near-infrared region of [2]catenanes **4**–**6** in the solid state (750–700 nm). (b) NIR Photothermal conversion curves of [2]catenanes **4**–**6** under 0.15 W/cm^2 laser irradiation at 730 nm.

tothermal conversion curves of [2]catenanes **4–6** under low power (0.15 W/cm^2) irradiation are shown in Fig. 9. [2]Catenane **4** (from 26.9 °C to 56.3 °C), **5** (from 26.3 °C to 53.1 °C), and **6** (from 27.1 °C to 51.2 °C) showed different temperature changes, higher than that of the corresponding complexes in solution. This feature reflects the outstanding stacking properties of [2]catenanes **4**–**6** in solid state. Furthermore, these results are comparable to those delivered by other top materials.

In summary, we have demonstrated that two types of supramolecular topological structures can be obtained by using different Cp*Rh based building blocks: metalla[2]catenanes and rectangular metallamacrocycles. Our studies have shown that π-π stacking interactions determine the selective synthesis of stable supramolecular topologies. Furthermore, efficient photothermal conversion can be observed by generating positive non-radiative pathways and suppressing radiative transition processes. Photothermal conversion of the prepared organometallic compounds in solution and solid state was studied. Under 660 nm and 0.6 W/cm^2, the conversion efficiencies of [2]catenane complexes **4**, **5** and **6** in solution were 18.8%, 17.1% and 16.5%, respectively. And that, the solid photothermal conversion study of [2]catenanes **4**, **5**, and **6** displayed the consistent warming trend with that observed in solution. Experimental data show that the synergistic effect of π-π stacking interactions, absorbance of the corresponding wavelength and conjugated effects of Cp*Rh building blocks result in different photothermal conversion efficiency. Studies on possible applications of [2]catenane complexes **4**, **5** and **6** in materials science are being carried out. These research not only inspire us to synthesize higher-order coordination supramolecular topologies, but also investigate their properties and application directionally.

Declaration of competing interests

The authors declare that they have no known competing financial interests or personal relationships that could have appeared to influence the work reported in this paper.

Acknowledgments

This work was supported by the National Natural Science Foundation of China (Nos. 22101108 and 22171123), and the Shanghai Science and Technology Committee (No. 19DZ2270100). training Plan for Young Core Teachers in Higher Education of Henan Province (No. 2021GGJS131), and Natural Science Foundation of Henan Province (No. 232300421232).

Supplementary materials

Supplementary material associated with this article can be found, in the online version, at doi:10.1016/j.cclet.2023.109298.

References

[1] N.L. Strutt, H.C. Zhang, S.T. Schneebeli, et al., Acc. Chem. Res. 47 (2014) 2631–2642.
[2] Z.L. Jiang, H. Zhao, J. Wang, et al., Chin. Chem. Lett. 34 (2023) 108334.
[3] W.P. Hu, Y. Wang, W.G. Zhu, et al., Angew. Chem. Int. Ed. 130 (2018) 4027–4031.
[4] T.R. Cook, Y.R. Zheng, P.J. Stang, Chem. Rev. 113 (2013) 734–777.
[5] E.R. Kay, D.A. Leigh, Angew. Chem. Int. Ed. 54 (2015) 10080–10088.
[6] M.C. Lipke, Y.L. Wu, I. Roy, et al., ACS Cent. Sci. 4 (2018) 362–371.
[7] X. Gao, Z. Cui, Y.R. Shen, et al., J. Am. Chem. Soc. 143 (2021) 17833–17842.
[8] F. Zeng, L.L. Tang, H. Yu, et al., Chin. Chem. Lett. 34 (2023) 108304.
[9] C.Q. Mu, Z.Y. Zhang, Y.L. Hou, et al., Angew. Chem. Int. Ed. 60 (2021) 12293–12297.
[10] H.L. Lu, J. Tong, H.W. Ma, et al., Chin. J. Struct. Chem. 40 (2021) 1680–1686.
[11] J. Singh, Kim, D.H. Singh, E.H. Kim, et al., J. Am. Chem. Soc. 142 (2020) 9327–9336.
[12] B.D. Nath, K. Takaishi, T. Ema, Catal. Sci. Technol. 10 (2020) 12–34.
[13] W.Q. Lv, Y.Y. Song, X.Y. Lv, et al., Chin. Chem. Lett. 34 (2023) 108179.
[14] S.J. Hu, X.Q. Guo, L.P. Zhou, et al., J. Am. Chem. Soc. 144 (2022) 4244–4253.
[15] Y.T. Wang, Y. Qin, X.L. Zhao, Chin. Chem. Lett. 34 (2023) 107576.
[16] L.X. Cai, D.N. Yan, P.M. Cheng, et al., J. Am. Chem. Soc. 143 (2021) 2016–2024.
[17] Y.H. Liu, Z.W. Guo, Y.C. Guo, et al., Chin. Chem. Lett. 34 (2023) 108531.
[18] S.C. Li, L.X. Cai, L.P. Zhou, et al., Sci. China Chem. 62 (2019) 713–718.
[19] S. Lu, D.J. Morrow, Z.K. Li, et al., J. Am. Chem. Soc. 145 (2023) 5191–5202.
[20] Y. Liu, S.H. Liao, W.T. Dai, et al., Angew. Chem. Int. Ed. 62 (2023) e202217215.
[21] C.D. Allen, A.James Link, J. Am. Chem. Soc. 138 (2016) 14214–14217.
[22] Z.W. Wang, L. Mei, C.X. Guo, et al., Angew. Chem. Int. Ed. 62 (2023) e202216690.
[23] N. Ponnuswamy, F.B.L. Cougnon, G.D. Pantos, et al., J. Am. Chem. Soc. 136 (2014) 8243–8251.
[24] Y.W. Zhang, S. Bai, Y.Y. Wang, et al., J. Am. Chem. Soc. 142 (2020) 13614–13621.
[25] D.A. Leigh, L. Pirvu, F. Schaufelberger, J. Am. Chem. Soc. 141 (2019) 6054–6059.
[26] L. Zhang, A.J. Stephens, A.L. Nussbaumer, et al., Nat. Chem. 10 (2018) 1083–1088.
[27] D.A. Leigh, J.J. Danon, S.D.P. Fielden, et al., Nat. Chem. 13 (2021) 117–122.
[28] W.X. Gao, H.J. Feng, B.B. Guo, et al., Chem. Rev. 120 (2020) 6288–6325.
[29] R. Chakrabarty, P.S. Mukherjee, P.J. Stang, Chem. Rev. 111 (2011) 6810–6918.
[30] P.J. Stang, J. Org. Chem. 74 (2009) 2–20.
[31] M. Fujita, M. Tominaga, A. Hori, et al., Acc. Chem. Res. 38 (2005) 369–378.
[32] D.L. Caulder, C. Brϵuckner, R.E. Powers, et al., J. Am. Chem. Soc. 123 (2001) 8923–8938.
[33] X.R. Liu, P.F. Cui, S.T. Guo, et al., J. Am. Chem. Soc. 145 (2023) 8569–8575.
[34] Z. Cui, Q.S. Mu, X. Gao, et al., J. Am. Chem. Soc. 145 (2023) 725–731.
[35] L.L. Dang, T.T. Zhang, T. Chen, et al., Angew. Chem. Int. Ed. 62 (2023) e202301516.
[36] Z. Cui, X. Gao, Y.J. Lin, et al., J. Am. Chem. Soc. 144 (2022) 2379–2386.
[37] S.L. Huang, Y.J. Lin, T.S.A. Hor, et al., J. Am. Chem. Soc. 135 (2013) 8125–8128.
[38] T. Feng, X. Li, Y.Y. An, Angew. Chem. Int. Ed. 59 (2020) 13516–13520.
[39] Z.E. Zhang, Y.F. Zhang, Y.Z. Zhang, et al., J. Am. Chem. Soc. 145 (2023) 7446–7453.
[40] W.L. Shan, Y.J. Lin, F.E. Hahn, et al., Angew. Chem. Int. Ed. 58 (2019) 5882–5886.

[41] L. Xu, D.W. Zhang, T.K. Ronson, et al., Angew. Chem. Int. Ed. 59 (2020) 7435–7438.
[42] E.G. Percástegui, T.K. Ronson, J.R. Nitschke, Chem. Rev. 120 (2020) 13480–13544.
[43] P.R. Su, B.W. Wei, C.X. Guo, et al., J. Am. Chem. Soc. 145 (2023) 3131–3145.
[44] J.K. Zhu, X.J. Chen, X. Jin, et al., Chin. Chem. Lett. 34 (2023) 108002.
[45] H.H. Duan, T. Yang, Q.F. Li, et al., Chin. Chem. Lett. 35 (2024) 108878.
[46] Y.J. Liu, P. Bhattarai, Z.F. Dai, et al., Chem. Soc. Rev. 48 (2019) 2053–2108.
[47] Y.Y. Li, J. Wang, F. Zhao, et al., Natl. Sci. Rev. 5 (2018) 365–388.
[48] Q.L. Zou, M. Abbas, L.Y. Zhao, et al., J. Am. Chem. Soc. 139 (2017) 1921–1927.
[49] L.L. Dang, T.T. Zhang, T. Chen, et al., Org. Chem. Front. 9 (2022) 5505–5515.
[50] W.X. Gao, H.N. Zhang, G.X. Jin, Coord. Chem. Rev. 386 (2019) 69–84.
[51] Y. Lu, D. Liu, Y.J. Lin, et al., J. Am. Chem. Soc. 143 (2021) 12404–12411.
[52] Q.L.S. Wang, Y.J. Lin, G.X. Jin, Chem. Commun. 57 (2021) 9772–9775.
[53] W.B. Yu, F.Y. Qiu, S.T. Luo, Inorg. Chem. Front. 8 (2021) 2356–2364.
[54] Y. Wang, W. Zhu, W. Du, et al., Angew. Chem. Int. Ed. 57 (2018) 3963–3967.
[55] L.B. Meng, W.Y. Zhang, D.Q. Li, et al., Chem. Commun. 51 (2015) 14381–14384.
[56] C.X. Sun, L. Wen, J.F. Zeng, et al., Biomaterials 91 (2016) 81–89.
[57] K.Y. Wang, M.Z. Zuo, T. Zhang, et al., Chin. Chem. Lett. 34 (2023) 107848.
[58] L.L. Dang, T.T. Li, T.T. Zhang, et al., Chem. Sci. 13 (2022) 5130–5140.
[59] B.L. Xue, X.W. Geng, H.H. Cui, et al., Chin. Chem. Lett. 34 (2023) 108140.
[60] M.Z. Zuo, T.H. Li, H.H. Feng, et al., Small 20 (2024) 2306746.